Technical Note

Variation in the mechanical properties of tracheal tubes in the American cockroach

Winston R Becker[1], Matthew R Webster[1], John J Socha[2] and Raffaella De Vita[1]

[1] Mechanics of Soft Biological Systems Laboratory, Department of Engineering Science and Mechanics, Virginia Tech, Blacksburg, VA 24061, USA
[2] Department of Engineering Science and Mechanics, Virginia Tech, Blacksburg, VA 24061, USA

E-mail: wbecker@vt.edu, mwbstr@vt.edu, jjsocha@vt.edu and devita@vt.edu

Abstract

The insect cuticle serves the protective role of skin and the supportive role of the skeleton while being lightweight and flexible to facilitate flight. The smart design of the cuticle confers camouflage, thermo-regulation, communication, self-cleaning, and anti-wetting properties to insects. The mechanical behavior of the internal cuticle of the insect in tracheae remains largely unexplored due to their small size. In order to characterize the material properties of insect tracheae and understand their role during insect respiration, we conducted tensile tests on ring sections of tracheal tubes of American cockroaches (*Periplaneta americana*). A total of 33 ring specimens collected from 14 tracheae from the upper thorax of the insects were successfully tested. The ultimate tensile strength (22.6 ± 13.3 MPa), ultimate strain ($1.57 \pm 0.68\%$), elastic modulus (1740 ± 840 MPa), and toughness (0.175 ± 0.156 MJ m^{-3}) were measured. We examined the high variance in mechanical properties statistically and demonstrated that ring sections excised from the same trachea exhibit comparable mechanical properties. Our results will form the basis for future studies aimed at determining the structure–function relationship of insect tracheal tubes, ultimately inspiring the design of multi-functional materials and structures.

Keywords: variation, mechanical properties, tensile tests, insect tracheal tubes, American cockroach

(Some figures may appear in colour only in the online journal)

1. Introduction

The structural attributes of insects continue to intrigue many scientists and engineers due to their multi-functionality and clever design. The cuticle of the insect, for example, is a remarkable smart material. It serves the protective role of skin and the supportive role of the skeleton while remaining lightweight and flexible enough to facilitate flight [21]. In insects, the material design of the cuticle promotes camouflage [26], thermo-regulation [14], communication [11], self-cleaning and anti-wetting [22]. The structural and mechanical properties of the *external* cuticle of the insect have been

characterized to some extent [1, 3, 4, 10, 12, 20, 21]. However, little attention has been given to the *internal* cuticle of the insect. In particular, the material properties of the vast network of tracheal tubes within the insect body have been only recently studied [24].

The study of the constituent materials of insects has informed the design of several materials with multi-functional properties. By mimicking the unique optical properties of the cuticle of metallic woodboring beetles, a multilayer material has been fabricated for the creation of iridescent panels [19]. A novel material inspired by insect cuticle, called 'shrilk',

has been recently created [5]. This material, which is made of chitosan, is clear, biocompatible, biodegradable, micromoldable, and still exhibits an ultimate strength of 119 MPa. A chitosan-based sponge derived from fly larvae has also been inspired by the insect cuticle; this sponge has the potential to serve as an absorbable surgical hemostatic agent [8]. The wide range of materials inspired by the insect cuticle indicates that chitin-based biological systems will enable the realization of smart engineering systems that possess multi-functional properties. Unlike the external cuticle, the tracheal tubes of insects remain largely unexplored, perhaps due to their nature as internal structures with less obvious functional characteristics worth emulating.

The insect respiratory system employs an extensive network of tracheal tubes to effectively transport oxygen directly to every cell of the body. These tubes are made of an outer layer of epithelial cells and an inner layer of spirally- or circumferentially-wound folds called taenidia. The taenidia are composed of chitin fibers embedded in a protein-rich matrix. They provide structural support to the tracheal tubes, largely contributing to their material stiffness. Localized deformations of these chitin-based tubular structures during insect respiration have been observed in the past decade using synchrotron x-ray imaging [7, 17, 18, 23, 25]. Interestingly, only some portions of some tracheal tubes appear to deform during rhythmic tracheal compression (figure 1). These localized deformations, which contribute to the transport of oxygen within the insect body, may be due to variation in the structural and mechanical properties of the tracheae [18, 24]. To make well-informed attempts to engineer novel smart materials and structures that emulate the respiratory systems of insects, a comprehensive characterization of the unique mechanical properties of insect tracheae is needed. The mechanical behavior of the tracheal tubes must directly influence patterns of tube collapse, which in turn may produce multiple types of flow patterns within the tracheal system. These fluid transport mechanisms could inspire the development of new microfluidic networks for use in applications such as engineered tissue constructs.

We have recently conducted the first mechanical experiments to determine the tensile properties of insect tracheae [24]. Micrometer-sized ring sections of tracheal tubes of the American cockroach (*Periplaneta americana*) were tested by using a custom-built tensile testing system. The results revealed a large variation in mechanical properties that has been commonly reported for other biological materials, including chitin-based materials [10, 15, 1, 13]. In the early work by Hepburn and Chandler [10] the material properties of arthrodial membranes in several arthropods were found to exhibit large variation despite the efforts to control experimental variables such as specimen orientation, hydration, and temperature. The mean value of the elastic modulus of the head articulation cuticle of the beetle (*Pachnoda marginata*) has been reported by Barbakadze *et al* [1] to be 1.50 GPa with a standard deviation of 0.80 GPa. Large confidence intervals were also noted in the recent experimental study by Lomakin *et al* [13] on the mechanical properties of the elytra of the red flour beetle (*Tribolium castaneum*). For example, an elastic modulus of 37 ± 16 MPa was reported for untanned samples of the elytra of *Tribolium castaneum*.

Our first study on the tracheal tubes of cockroaches, together with previous studies of the exoskeleton, suggest the need for new experimental investigations that focus on identifying the origin of the large variation in the mechanical properties of chitin-based materials. These investigations will be crucial for interpreting accurately the mechanical behavior of these materials in relation to their physiological function.

In theory, the variation in mechanical properties of ring sections of tracheal tubes in insects can be attributed to biological differences among insects, differences among anatomical locations of tracheal tubes, and intrinsic structural differences within individual tracheal tubes. In this study, we examine the potential source of variation in mechanical properties of insect tracheae by performing tensile tests on ring sections from tracheal tubes of American cockroaches. We compare the properties in the main tracheal trunk on the left *versus* right side across multiple ring specimens. Additionally, we examine variation in mechanical properties for ring sections excised from the same tracheal tube.

2. Methods

Tracheal tubes were excised from adult male American cockroaches (*Periplaneta americana*), which were acquired from a colony in the Department of Entomology at Virginia Tech. The cockroaches were fed and watered *ad libitum* and kept in ambient conditions in a colony. Adult male cockroaches were sacrificed in fumes of ethyl acetate, the pronotum was removed, and the four main tracheal trunks in the thorax were extracted (figure 2(a)). These tracheal tubes were selected for their large diameter and length relative to other tubes in the roach. After extraction, the tracheal tubes were manually cut into ring sections with a scalpel. Two to three ring sections of approximately constant diameter were selected for mechanical testing from each trachea.

The tubes were immediately placed in a bath containing an insect-specific Ringer's solution (0.75 g NaCl, 0.35 g KCl, 0.28 g CaCl$_2$, 1 l distilled water), and were stored until testing. Prior to testing, the width and thickness of the ring sections were measured in ProAnalyst (Xcitex ProAnalyst, Xcitex Inc., Cambridge, MA, USA) using images obtained from a digital camera (Nikon D-5000, Nikon Inc., Tokyo, Japan). The measurement error was determined to be ± 0.2 μm based on the camera resolution (4288×2848) and the level of magnification of the stereoscope ($30\times$). To produce suitable contrast for strain measurements, the surface of the ring specimens was speckle-coated with black ink using an airbrush (Badger Model 150, Badger Air-Brush Co., Franklin Park, IL, USA).

The specimens were tested with a custom-built tensile testing device (figure 3). Custom grips were built to hold the specimens during testing. The grips were primarily made of polycarbonate, two 150 μm diameter tungsten wires, and two $19.0 \times 9.52 \times 1.58$ mm^3 magnetic plates. The design of the grips is described in detail elsewhere [24]. During testing, the two tungsten wires were threaded through each side of the ring specimens as shown in the insert of figure 3. The load was measured using a load cell (LSB200 JR S-Beam
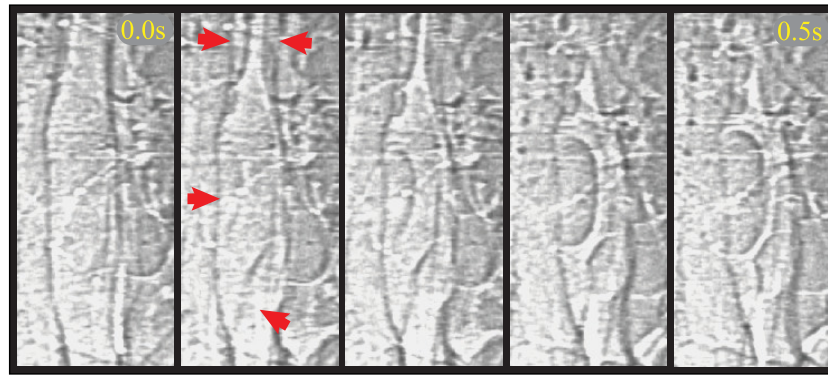
Figure 1. Representative compression of a tracheal tube in an insect, progressing from left ($t = 0$ s) to right ($t = 0.5$ s). The red arrows indicate locations where compression was initiated, resulting in a dimpled pattern of collapse across the cylindrical tube. The initial diameter of the tube was 50 μm. This tube was from an unidentified beetle of the family Carabidae and was imaged with synchrotron x-rays at the Advanced Photon Source, Argonne National Laboratory. See [17] for details of imaging methodology.
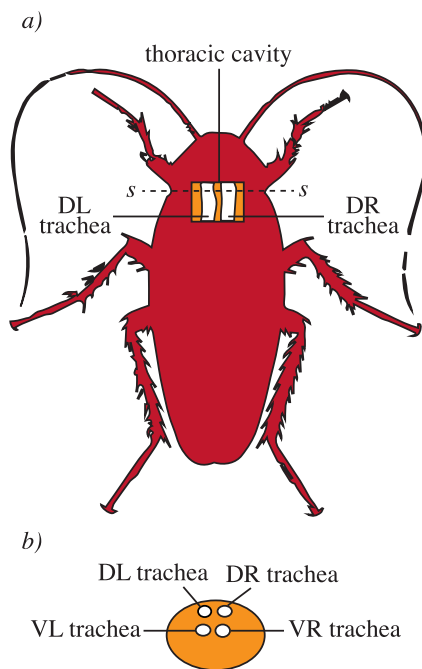

Figure 2. Schematic of the American cockroach and the four main thoracic tracheal trunks. (a) Top view of the dorsal right (DR) and dorsal left (DL) tracheae. (b) Cross sectional view of the dorsal right (DR), dorsal left (DL), ventral right (VR), and ventral left (VL) tracheae. (a) Top view. (b) Cross section s–s.

Load Cell, FUTEK Advanced Sensor Technology Inc., Irvine, CA, USA) with a maximum capacity of 50 g and accuracy of ±0.075 g. The specimens were displaced until failure using a microscale linear actuator (Zaber T-NA, Zaber Technologies Inc., Vancouver, British Columbia) at a displacement rate of 2.5 μm s^{-1}. This low displacement rate was selected to ensure quasi-static loading of the specimens.

The specimens were submerged in a bath of Ringer's solution to maintain hydration during testing. The bath was placed under a microscope (Wild Heerbrugg M3Z, Wild Heerbrugg AG, Switzerland) with 40× magnification and illuminated via two LED lamps (SCHOTT North America Inc.,

Southbridge, MA, USA). The deformation of the specimen was recorded using a CCD camera (Stingray, Allied Vision Technologies Inc., Newburyport, MA, USA) at a rate of 25 fps and image size of 1032 px × 776 px, with a field of view of roughly 1.2 mm × 1.4 mm. Images, force, and displacement data were recorded synchronously at 25 Hz to a desktop computer via a data acquisition module (NI cDAQ-9172, National Instruments Inc., Austin, TX, USA) using LabVIEW software (LabVIEW 2010, National Instruments Inc., Austin, TX, USA).

Prior to testing, a preload (avg. = 0.003 N) was applied to flatten the initially bent ring specimens and to prevent out-of-plane motion during testing. Nominal stress and engineering strain data were computed by choosing the preloaded configuration as the reference configuration. Engineering strain of the ring sections was determined during each test using a digital image correlation (DIC) method implemented in Matlab (Version 7.12.0, MathWorks Inc., Natick, MA, USA). For these tests, strain values were calculated from a rectangular grid consisting of at least 30 points located at the center of the specimen. The nominal stress, σ, was calculated as:

$$\sigma = \frac{L}{2tw} \qquad (1)$$

where L, t, and w are the load, thickness, and width of the specimen, respectively. The stress and strain data were smoothed using 3- and 19-point running averages, respectively. The calculated stress and strain values were used to determine the elastic modulus, ultimate tensile strength, ultimate strain, and toughness of each specimen. The elastic modulus was calculated as the slope of the stress–strain curve. In cases where nonlinear behavior was observed, the elastic modulus was calculated from the linear region of the stress–strain curve. The ultimate tensile strength and ultimate strain were calculated as the magnitude of stress and strain, respectively, before the load was observed to decrease, indicating the occurrence of damage in the specimens. Toughness was measured by calculating the area under the stress–strain curve using a trapezoidal numerical integration scheme (*trapz* function) implemented in Matlab.
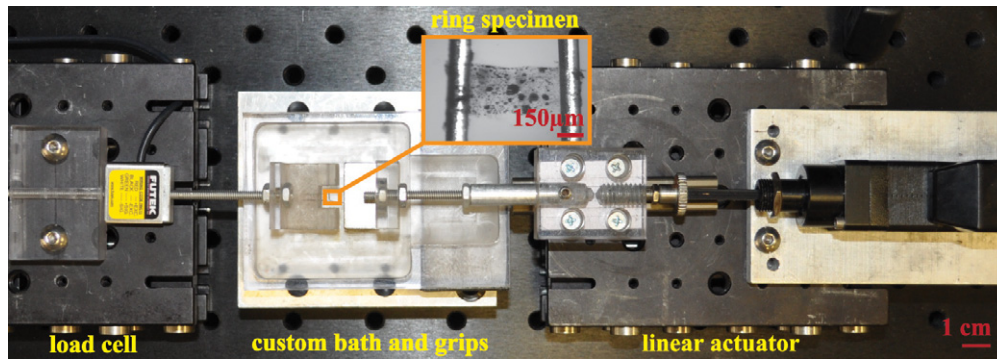
Figure 3. Experimental setup used for testing ring specimens of insect tracheal tubes.

In some cases, shearing stress, concentrated loading, and out-of-plane motion were observed during testing. The results of these tests were not included in the analysis of the data. Often, although more than two ring sections from an individual tracheal tube were selected for testing, only one ring section was tested successfully. In these cases, the results of the tests were also discarded because the data were irrelevant to this study, which focused on quantifying the variance of mechanical properties of ring sections isolated from the same tracheal tubes. A total of 140 ring sections were prepared and 80 were tested. A sample size of 33 ring sections, from 14 tracheal tubes (from 11 roaches) met the above-described criteria for analysis. More specifically, 14 ring sections were from the dorsal right (DR), 14 from the dorsal left (DL), 3 from the ventral right (VR), and 2 from the ventral left (VL) tracheae (figure 2(b)).

From the experimental data, four data sets, one for each of the mechanical properties, were obtained. The statistical analysis of each data set was conducted using Matlab. The mean, standard deviation, and variance were computed for the mechanical properties measured by testing all the specimens ($n = 33$). The comparison of mechanical properties between ring sections extracted from the DR and VL tracheal tubes was performed by employing the *Student's t-test* with a significance level of 0.05 ($p \leq 0.05$).

The bootstrap method was employed to obtain estimates of the variances of the mechanical properties of the entire population of tracheae, which are impossible to test experimentally, from a sample of 33 ring sections [2]. By using the bootstrap method, the elastic modulus, ultimate tensile strength, ultimate strain and toughness computed from the 33 test ring sections were resampled 10 000 times. From each resample, the variance was computed, thus generating a histogram that provided an approximate distribution of the variance of the population. This distribution was needed to evaluate statistically the variance of ring sections from the same trachea in relation to the variance of the entire population.

For each mechanical property, the experimentally measured variance of specimens prepared from the same tracheal tube was compared with the bootstrap-generated distribution of the variance of the population (figure 4). Toward this end, the probability of obtaining a higher variance from ring sections of the same trachea within the entire population was computed.

For the jth tracheal tube, where $j = 1 \ldots 14$, this probability, denoted by p_j, was computed using the following equation:

$$p_j = \frac{1}{N} \sum_{i=1}^{N} \gamma_i \qquad \text{with } \gamma_i = \begin{cases} 1 & \text{if } v_j^{\text{tube}} \geq v_i \\ 0 & \text{if } v_j^{\text{tube}} < v_i \end{cases} \quad (2)$$

where $N = 10\,000$ is the number of times the data were resampled, v_i is the variance of the mechanical property of the ith resampled data set, and v_j^{tube} is the variance of the mechanical property computed from specimens extracted from the jth tube. The α-value adopted in this analysis was set to 0.05 so that, for a probability p_j less than the α-value of 0.05, v_j^{tube} was significantly lower than the variance of the overall population. Because we computed four mechanical properties from each of the 14 tested tubes, such comparisons were performed a total of 56 times.
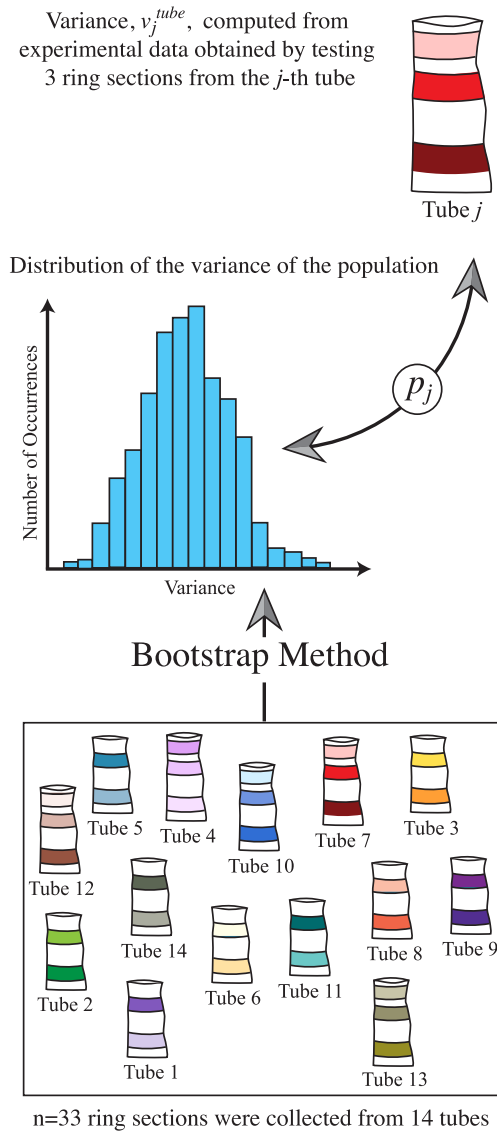
3. Results

Linear and nonlinear stress–strain curves were obtained by analyzing the experimental data collected from ring sections of tracheal tubes in the American cockroaches. In figure 5, two representative stress–strain curves which show this remarkable difference are presented. The curvature of the stress–strain curve did not depend on the anatomical location (e.g., dorsal left versus dorsal right) of the tracheae in the cockroach. However, such curvature was, in general, similar for ring sections isolated from the same tracheal tube.
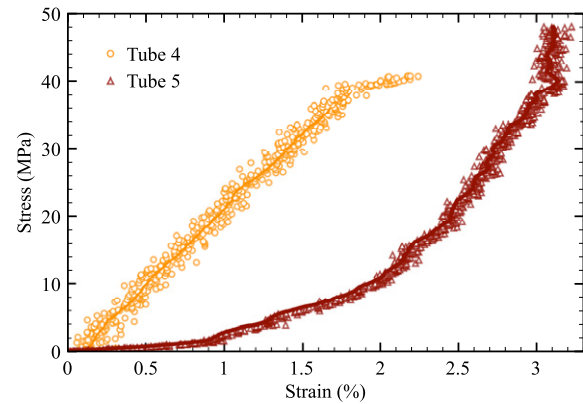
The nonlinear curves were concave up at low strain values and became linear as the strain increased. These tracheal tubes exhibited the characteristic strain stiffening behavior observed in many biological tissues: the elastic modulus increases with strain until partial or complete failure occurs. The overall mean, standard deviation, and variance for the mechanical properties computed experimentally from the 33 tested specimens are reported in table 1. Large standard deviations (and variances) were recorded for the elastic modulus, ultimate tensile strength, ultimate strain, and toughness, which indicates high levels of variability in these mechanical properties. For example, the mean value of the elastic modulus was 1740 MPa and the standard deviation was 840 MPa. This emphasizes the large range of possible values for the elastic modulus of these chitin-based materials.

Table 1. Mechanical properties of tracheal tubes computed from $n = 33$ specimens (width $= 0.46 \pm 0.11$ mm, thickness $= 0.0057 \pm 0.004$ mm).

Mechanical property	Mean	Standard deviation	Variance
Elastic modulus	1740 (MPa)	840 (MPa)	7.05×10^5 (MPa^2)
Ultimate tensile strength	22.6 (MPa)	13.3 (MPa)	176.9 (MPa^2)
Ultimate strain	1.57×10^{-2}	0.68×10^{-2}	0.462×10^{-4}
Toughness	0.175 (MJ m^{-3})	0.156 (MJ m^{-3})	0.0243 (MJ m^{-6})

Variance, v_j^{tube}, computed from experimental data obtained by testing 3 ring sections from the j-th tube

Tube j

Distribution of the variance of the population

p_j

Number of Occurrences

Variance

Bootstrap Method

Tube 5 Tube 4 Tube 7 Tube 3 Tube 10 Tube 12 Tube 14 Tube 8 Tube 9 Tube 2 Tube 6 Tube 11 Tube 1 Tube 13

n=33 ring sections were collected from 14 tubes

Figure 4. Schematic representation of the methods used to compare the experimentally measured variance of ring sections extracted from the same tracheal tube with the bootstrap-generated distribution of the variance of the population. Note that p_j is defined by equation (2).

The tensile properties of specimens isolated from the DL and DR tracheal tubes were compared statistically. In figure 6 the mean and the standard deviation of the tensile properties computed for 14 ring specimens taken from the DL and DR tracheal tubes are presented. This comparison was made to test for dependence of mechanical properties on the anatomical

Figure 5. Typical difference in the mechanical response of ring sections of tracheal tubes: linear elastic behavior (orange symbols) of a ring section extracted from Tube 4 and nonlinear elastic behavior (red symbols) for a ring section extracted from Tube 5. The continuous lines represent the smoothed data.

location of tracheal tubes. The specific anatomical locations were selected based on the largest number of specimens that we were able to isolate and test successfully. Using a *Student's t-test* with a significance level of 0.05, no statistical difference between the tensile properties of the DL and DR tracheae was observed ($p > 0.05$). For example, the elastic moduli (mean $\pm$ S.D.) were found to be 1850 ± 854 MPa and 1750 ± 828 MPa for the DL and DR tracheae, respectively.

Histograms presenting the approximate distribution of the variance computed using the bootstrap method for each mechanical property are shown in figure 7. On these histograms, the width of the bins represents the range of variances while the height of the bins represents the number of occurrences. The number of occurrences is the number of times in which the variance fell in each range of variances. Because the sample data were resampled 10 000 times, there are 10 000 total occurrences in each histogram. The variances computed experimentally from all the tested specimens ($n = 33$) in table 1 were found to be approximately equal to the bootstrap estimated variances at the largest number of occurrences. The results of the bootstrap method showed that the variance of the entire population can be lower and higher than the experimentally measured variance. For each mechanical property, the variance of each tube, v_j^{tube} for $j = 1 \ldots 14$, is also reported in figure 7 to compare it directly to the variance of the overall population.

The tensile properties of ring sections extracted from the same tracheal tubes were compared. It was found that these ring sections exhibited similar mechanical behavior. This can be observed qualitatively in figure 8 where the stress–strain
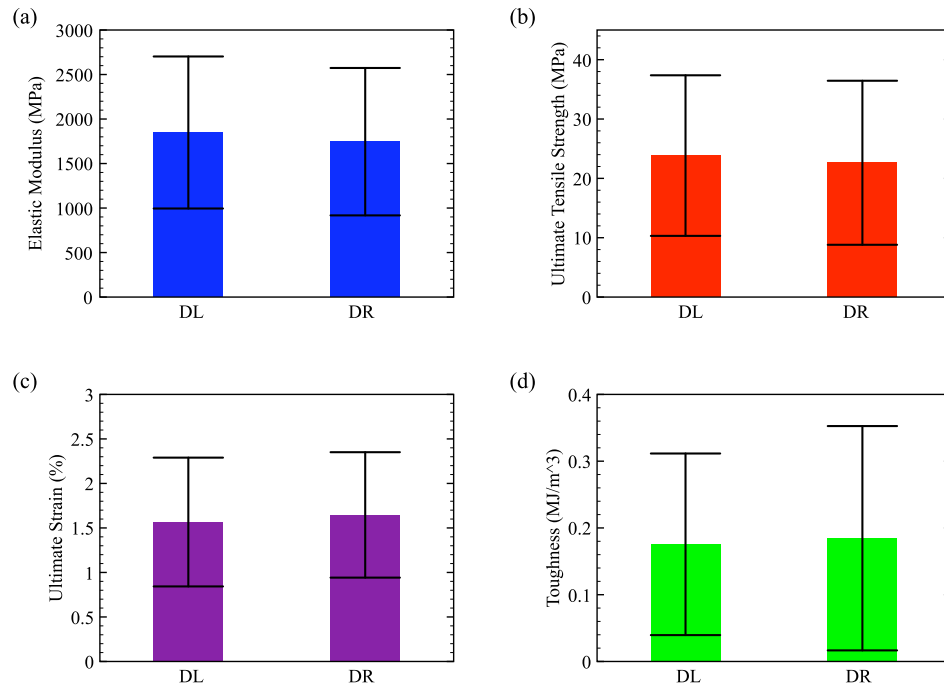
Figure 6. Tensile properties computed for the dorsal left (DL) ($n = 14$ ring specimens) and dorsal right (DR) ($n = 14$ ring specimens) main thoracic tracheal trunks ($p > 0.05$).
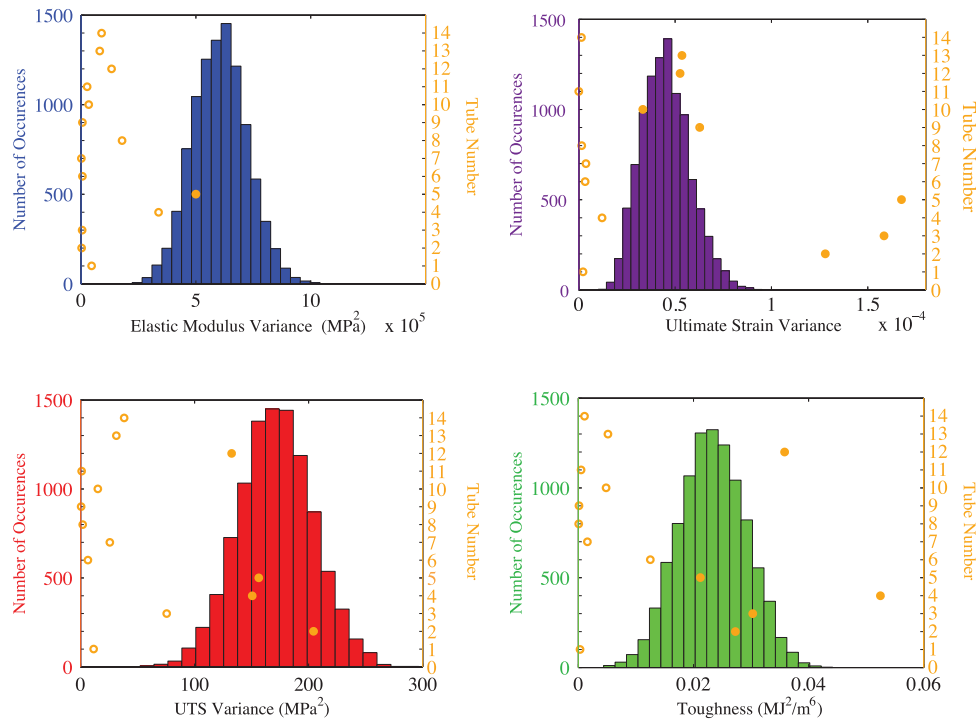

Figure 7. Histograms representing the distributions of the statistically generated estimates of variance for the elastic modulus, ultimate strain, ultimate tensile strength (UTS), and toughness. Circular symbols represent the experimentally measured variance of the mechanical properties for each tracheal tube (v_j^{tube} in equation (2)). Specifically, unfilled circular symbols denote experimentally measured variances that were significantly lower than the statistically generated estimates of variance of the overall population ($p_j < 0.05$).

curves of 10 ring sections obtained from 4 tracheal tubes are shown. It must be noted that, for clarity, only 10 out of the 33 stress–strain curves obtained in this experimental study are displayed. From figure 8, one can observe that specimens obtained from the same tracheal tubes had nearly identical stress–strain curves but failed at very different strains.
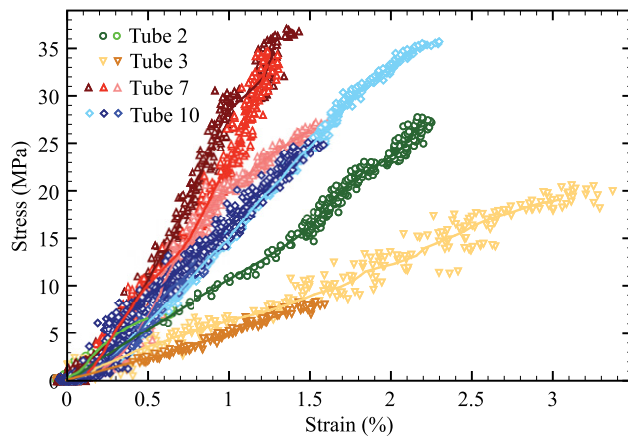
Figure 8. Stress–strain curves for 10 ring sections from 4 tracheal tubes. Symbols represent raw data and continuous lines represent smoothed data.

The variability in the mechanical properties of ring sections of single tracheal tubes is further demonstrated in figure 9. In this figure, the properties of the ring sections are plotted against the tracheal tube from which they were obtained. In particular, the values of the elastic modulus were nearly identical for some ring sections taken from the same tube (figure 9(a)). In figure 9, the results of the comparison of the experimentally computed variance for each tube with the variance of the population computed using the bootstrapping method are also presented. Unfilled circular symbols indicate that the variance of each tracheal tube was significantly lower than the variance of the overall population. As indicated by the plots, the variance was significantly lower for 13 of 14 tubes for the elastic modulus (figure 9(a)), 10 of 14 tubes for the ultimate tensile strength (figure 9(b)), 7 of 14 tubes for the ultimate strain (figure 9(c)), and 9 of 14 tubes for the toughness (figure 9(d)).

The tracheal tubes exhibited significantly less variation in the elastic modulus than the other material properties. This is a consequence of the similar shape of the stress–strain curves for specimens taken from the same locations (figure 8). Because the ring sections failed at different strains, the other tensile properties that are affected by the strain at failure show larger variation. For example, elastic moduli of 1223 and 1295 MPa were computed for the two ring sections of Tube 2 (figure 9(a)). Although the values of the elastic modulus were comparable, the values of the ultimate tensile strength (27.8 and 7.54 MPa in figure 9(b)), ultimate strain (0.0224 and 0.0064 in figure 9(c)), and toughness (0.263 and 0.0293 MJ m^{-3} in figure 9(d)) were found to be quite different for Tube 2. A similar result was found for Tube 12: a significantly lower variance was recorded for the elastic modulus, but not for any of the other tensile properties. In the case of Tube 2, the largest variation in the mechanical properties was observed for the toughness, which differed by approximately one order of magnitude. Toughness was calculated as the area under the entire stress–strain curve. Consequently, the variation measured in both the ultimate tensile strength and ultimate strain was amplified when computing the toughness.

4. Discussion

In this study, we explored the variation in mechanical properties of insect tracheal tubes in one species. We tested micrometer-sized ring sections of tracheal tubes extracted from American cockroaches with a custom-built tensile testing device. Unlike a previous study [24], experimental data were collected and analyzed only when two to three ring sections from individual tracheal tubes were excised from the insects and successfully tested. Overall, large amounts of variation in the elastic modulus, ultimate tensile strength, ultimate strain, and toughness of tracheal tubes were observed (table 1). These findings were consistent with our previous study as well as many experimental studies on the insect cuticle [10, 15, 1, 13]. The values of the measured mechanical quantities were comparable to those reported for other types of insect cuticle [1].

High variation in the material properties was also noted when the experimental data were collected from ring sections excised from the same anatomical locations in different animals (figure 6). The DR and DL tracheal tubes in the upper thorax of the cockroach, as shown in figure 2, were selected. There was no significant difference between the tensile properties of tracheal tubes at these anatomical locations, which demonstrates the symmetry between the left and right sides of the tracheal system.

Qualitatively, stress–strain curves of ring specimens taken from the same tracheal tube had roughly the same curvature (i.e. the curves were generally either all linear or all nonlinear for ring specimens obtained from the same tube) (figure 8). What is not clear is why some of the specimens exhibit linear elastic behavior while others exhibit nonlinear elastic behavior. This discrepancy likely results from microstructural differences existing among tracheal tubes. We are currently conducting scanning electron microscopy studies to understand the origin of such variations. Our preliminary investigations seem to indicate that inter-taenidia spacing and taenidia bifurcations may play a key role in the different material behaviors observed.

The distributions of the statistically generated estimates of variance for each mechanical property are presented by the histograms in figure 7. The experimentally measured values of variance for each tube are represented by points in the same figure. Figure 7 demonstrates that the experimentally measured variances are, in most cases, lower than the statistically generated estimates of variance. There are, however, some exceptions: the experimentally measured variances of the ultimate strain and toughness were higher than the statistically determined variance for three tracheae (Tube 2, Tube 3, Tube 5) and one trachea (Tube 4), respectively. These results are due to the large differences in failure strains at which the ring sections from these tracheae failed. We speculate that these large differences may be determined by small imperfections, tears, or changes in structure that were not detectable in the specimens prior to mechanical testing.

It must be noted that there is inevitable technical variability in the results of any experiment. Many factors contribute to such variability including human error, daily changes in the
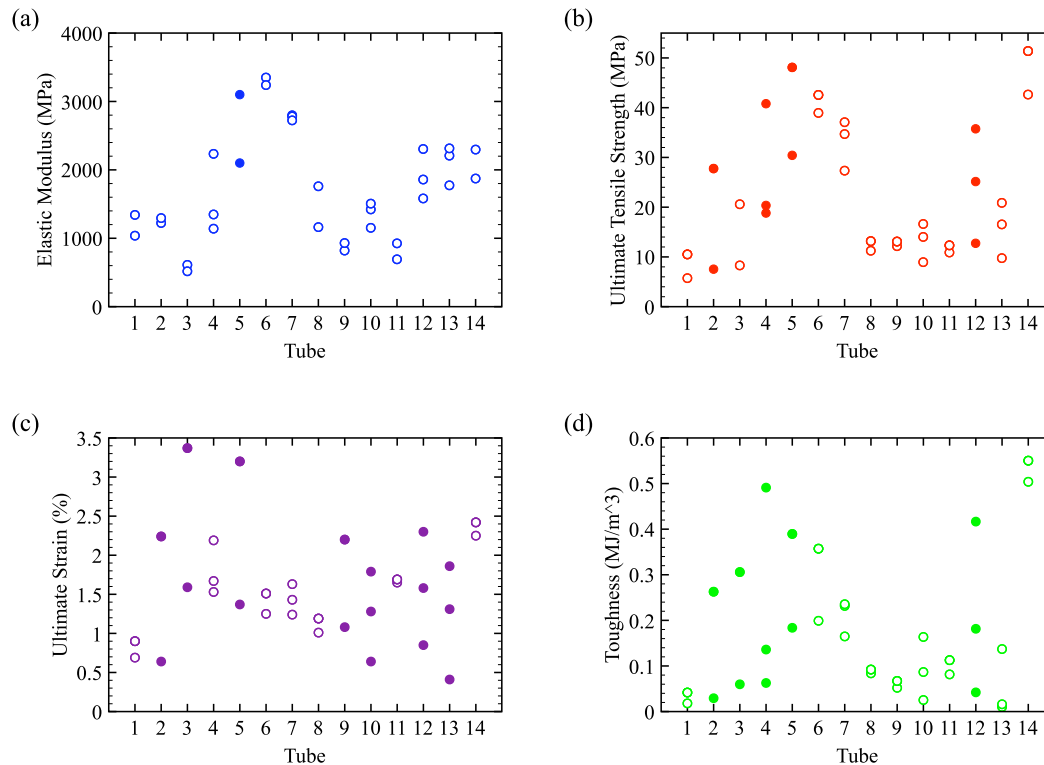
Figure 9. Tensile properties of ring specimens presented versus the tube from which they were obtained. Note that two to three ring sections were excised from each tracheal tube. Unfilled circular symbols indicate that the variance of the properties for ring sections of an individual tracheal tube, v_j^{tube}, is significantly lower than the variance of the overall population ($p_j < 0.05$) while, on the contrary, filled circular symbols indicate that such variance was not significantly lower than the variance of the overall population ($p_j \geq 0.05$).

testing environment, and reliability of the testing equipment. In this study, we assumed that these factors affected every measurement equally. Under these assumptions, the mechanical tests and statistical analysis provide evidence that the tensile properties are more consistent within a single tracheal tube than among different tracheal tubes. These findings may offer insight into the function of the insect tracheal system and, more specifically, the rhythmic tracheal compression [18]. Indeed, with respect to insect physiology, our results may explain why some tracheal tubes deform during respiration while others remain inflated, as recently observed in the American locust Schistocerca americana [9]. Further research is needed to determine the structural differences among tracheal tubes that perform different functions during insect respiration.

The outcome of this investigation will aid the design of micro-structural studies that reveal the origin of the variation in the mechanical properties of tracheal tubes in the American cockroach. By performing mechanical tests on one section of the tracheal tube and micro-structural analysis on other sections, which we now know have similar mechanical properties, the relationship between the structure and mechanics of these tube will be unraveled. Mechanical experiments conducted in tandem with micro-structural studies will elucidate the role of the structural components of the tracheae in determining the linear and nonlinear elastic behavior. Developing an understanding of the structure–function relationship in insect tracheal systems will facilitate the design of multi-functional

materials and structures that emulate the collapse and re-inflation characteristics of this system.

5. Conclusions

The experimental data and statistical analysis demonstrate that, for American cockroaches, the variance of tensile properties for ring specimens extracted from the same trachea is lower than the variance that is statistically computed using the bootstrap method from all tested tracheal tubes. Simply put, two ring sections extracted from a single trachea are likely to have more comparable values of tensile properties than two ring sections extracted from two different tracheae.

Acknowledgments

References

[1] Barbakadze N, Enders S, Gorb S and Arzt E 2006 Local mechanical properties of the head articulation cuticle in the

beetle *Pachnoda marginata* (Coleoptera, Scarabaeidae) *J. Exp. Biol.* **209** 722–30

[2] Chernick M R 2007 *Bootstrap Methods: A Guide for Practitioners and Researchers* (Hoboken, NJ: Wiley)

[3] Dirks J H and Taylor D 2012 Fracture toughness of locust cuticle *J. Exp. Biol.* **215** 1502–8

[4] Dirks J H, Parle E and Taylor D 2013 Fatigue of insect cuticle *J. Exp. Biol.* **216** 1924–7

[5] Fernandez J G and Ingber D E 2012 Unexpected strength and toughness in chitosan-fibroin laminates inspired by insect cuticle *Adv. Mater.* **24** 480–4

[6] Fratzl P 2007 Biomimetic materials research: what can we really learn from nature's structural materials? *J. R. Soc. Interface* **4** 637–42

[7] Greenlee K J, Socha J J, Eubanks H B, Pedersen P, Lee W K and Kirkton S D 2013 Hypoxia-induced compression in the tracheal system of the tobacco hornworm caterpillar, *Manduca sexta J. Exp. Biol.* **216** 2293–301

[8] Gu R, Sun W, Zhou H, Wu Z, Meng Z, Zhu X, Tang Q, Dong J and Dou G 2010 The performance of a fly-larva shell-derived chitosan sponge as an absorbable surgical hemostatic agent *Biomaterials* **31** 1270–7

[9] Harrison J F, Waters J S, Cease A J, VandenBrooks J M, Callier V, Klok C J, Shaffer K S and Socha J J 2013 How locusts breathe *Physiology* **28** 18–27

[10] Hepburn H R and Chandler H G 1976 Material properties of arthropod cuticles: the arthrodial membranes *J. Comp. Physiol.* **109** 177–98

[11] Howard R H 1993 Cuticular hydrocarbons and chemical communication *Insect Lipids: Chemistry, Biochemistry and Biology* (Lincoln, NE: University of Nebraska Press) pp 179–226

[12] Jensen M and Weis-Fogh T 1962 Biology and physics of locust flight. V. Strength and elasticity of locust cuticle *Phil. Trans. R. Soc. Lond.* B **245** 137–69

[13] Lomakin J, Huber P A, Eichler C, Arakane Y, Kramer K J, Beeman R W, Kanost M R and Gehrke S H 2011 Mechanical properties of the beetle elytron, a biological composite material *Biomacromolecules* **12** 321–35

[14] May M L 1979 Insect thermoregulation *Annu. Rev. Entomol.* **24** 313–49

[15] Melnick C A, Chen Z and Mecholsky J J 1996 Hardness and toughness of exoskeleton material in the stone crab, Menippe mercenaria *J. Mater. Res.* **11** 2903–7

[16] Rajesh S, O'Carroll D and Abbott D 2005 Man-made velocity estimators based on insect vision *Smart Mater. Struct.* **14** 413–24

[17] Socha J J, Westneat M W, Harrison J F, Waters J S and Lee W K 2007 Real-time phase-contrast x-ray imaging: a new technique for the study of animal form and function *BMC Biol.* **5** 6

[18] Socha J J, Westneat M W, Harrison J F, Waters J S and Lee W K 2008 Correlated patterns of tracheal compression and convective gas exchange in a carabid beetle *J. Exp. Biol.* **211** 3409–20

[19] Vigneron J P, Rassart M, Lousse V, Deparis O, Biro L P, Dedouaire D, Cornet A and Defrance P 2006 Spectral filtering of visible light by the cuticle of metallic woodboring beetles and microfabrication of a matching bioinspired material *Phys. Rev.* E **73** 041905

[20] Vincent J F V 2002 Arthropod cuticle: a natural composite shell system *Compos. Appl. Sci. Manuf.* **33** 1311–5

[21] Vincent J F V and Wegst U G K 2004 Design and mechanical properties of insect cuticle *Arthropod Struct. Dev.* **33** 187–99

[22] Wagner T, Neinhuis C and Barthlott W 1996 Wettability and contaminability of insect wings as a function of their surface sculptures *Acta Zool.* **77** 213–25

[23] Waters J S, Lee W K, Westneat M W and Socha J J 2013 Dynamics of tracheal compression in the horned passalus beetle *Am. J. Physiol. Regul. Integr. Comp. Physiol.* **8** 621–7

[24] Webster M R, De Vita R, Twigg J N and Socha J J 2011 Mechanical properties of tracheal tubes in the American cockroach (*Periplaneta americana*) *Smart Mater. Struct.* **20** 094017

[25] Westneat M W, Betz O, Blob R W, Fezzaa K, Cooper W J and Lee W K 2003 Tracheal respiration in insects visualized with synchrotron x-ray imaging *Science* **298** 558–60

[26] Wilts B D, Michielsen K, Kuipers J, De Raedt H and Stavenga D G 2012 Brilliant camouflage: photonic crystals in the diamond weevil, Entimus imperialis *Proc. R. Soc.* B **279** 2524–30